ELSEVIER

Journal of Photochemistry and Photobiology A: Chemistry 132 (2000) 225–232

Journal of Photochemistry and Photobiology A:Chemistry

www.elsevier.nl/locate/jphotochem

VOC photodegradation at the gas–solid interface of a TiO_2 photocatalyst Part I: 1-butanol and 1-butylamine

Florence Benoit-Marquié [a,*], Uwe Wilkenhöner [a], Valérie Simon [b], André M. Braun [c], Esther Oliveros [c], Marie-Thérèse Maurette [a]

[a] *Laboratoire des IMRCP, UMR 5623, Université Paul Sabatier, F-31062 Toulouse Cedex, France*

[b] *Ecole Nationale Supérieure de Chimie, 118 route de Narbonne, F-31077 Toulouse, France*

[c] *Lehrstuhl für Umweltmesstechnik, Engler-Bunte-Institut, Universität Karlsruhe, D-76128 Karlsruhe, Germany*

Received 25 August 1999; accepted 13 December 1999

Abstract

The gas–solid heterogeneous photocatalytic oxidation of 1-butanol and 1-butylamine in air was investigated using supported TiO_2 as a catalyst. The supported catalyst was prepared using a sol–gel method and irradiated employing two different light sources, a medium pressure mercury lamp or a xenon-chloride excimer lamp. The experimental set-up was especially designed for generating a gas stream containing stable and defined concentrations of the model pollutants. The gas stream at the reactor exit was analyzed on line by gas chromatography and the structures of the intermediates were established by gas chromatography coupled with mass spectrometry. Six major intermediates (butanal, butanoic acid, 1-propanol, propanal, ethanol and ethanal) were identified in the case of the photocatalytic degradation of 1-butanol. 1-Butylamine was less efficiently adsorbed on the catalyst and its degradation was slower. Three intermediates could be identified in this case (*N*-butylidene-1-butylamine, *N*-ethylidene-1-butylamine and *N*–butylformamide). Based on these results, a degradation mechanism is proposed for both compounds. Mineralization could be achieved under various conditions of concentrations and flow rates and was confirmed by infrared spectroscopy.

Keywords: Photocatalytic degradation; TiO_2; Gas phase; Excimer lamp; 1-Butanol; 1-Butylamine

1. Introduction

Remediation of volatile organic compounds (VOC) has become a major area of investigation in environmental protection during the last decade. Adsorption (on activated carbon or zeolites) or scrubbing are the most current recovery processes but further treatments are required to regenerate the supports and dispose off the organic matter. Complete degradation of toxic organic contaminants may only be achieved by incineration or chemical treatment. Photochemical degradation processes (also referred to as advanced oxidation processes, AOP) have become increasingly popular as alternative or complementary treatments [1,2]. Several AOPs have been investigated for VOC abatement, including UV photolysis, H_2O_2/UV, O_3/UV, H_2O_2/O_3/UV (see e.g., [3–5]) photocatalysis [2] and more recently, vacuum ultraviolet (V-UV) photolysis using a new type of light sources (Xe-excimer lamps) [6–8]. Solid–gas phase heterogeneous photocatalysis using TiO_2 has attracted considerable interest for VOC removal, in particular due to the possible use of solar radiation, and numerous applications have been proposed [9–11]. A large variety of organic compounds may be oxidized by TiO_2 photocatalysis in the presence of molecular oxygen. For instance, Péral and Ollis [12] studied in a project on air quality the photocatalyzed oxidation of oxygenated compounds, such as acetone, 1-butanol (BU), butanal, formaldehyde and *m*-xylene, detected at working places (offices, workshops). Suzuki [13] applied photocatalytic oxidation to achieve elimination of odors and studied, in particular, the degradation of organic compounds such as ethanal, butanoic acid, toluene, methylmercaptan, triethylamine. We have been interested in the photocatalytic degradation of aliphatic compounds bearing an alcohol or amine function and we have chosen BU and 1-butylamine (BA) as model compounds. The first authors who studied the degradation of BU could only identify butanal as an intermediate [14,15]. Blake and Griffin [14] proposed the parallel formation of butene. However, this hypothesis was invalidated by the work of Peral and Ollis who could not detect this compound, and the mechanism for the oxidative

* Corresponding author.

1010-6030/00/$ – see front matter
PII: S1010-6030(00)00196-9

degradation of BU by photocatalysis has not been established so far. Up to now, very few studies have been carried out on amines and none of them suggests a degradation mechanism [16]. In this work, photocatalytic degradation of BU and BA was performed using two different types of light sources: a medium pressure mercury arc (polychromatic irradiation) and a xenon-chloride excimer lamp emitting at 308 nm. Experimental conditions for complete degradation of these substances were established and a reaction mechanism is proposed.

2. Experimental details

2.1. Experimental set-up

A schematic representation of the experimental set-up used for performing photocatalytic degradation processes at the solid–gas interface is given in Fig. 1. It includes three parts: generation of a defined gas mixture containing the organic substrate, photochemical reactor and on-line analytical equipment.

The gas mixture containing a defined and stable concentration of the compound used as a model pollutant (BU and BA) was generated using a diffusion cell [17]. This cell consisted of a reservoir containing the pure (liquid) polluting agent and linked to a mixing flask by means of a capillary tube of characteristic diameter and length. Reservoir and capillary tube were both immersed in a thermoregulated bath. The flow rate of the gas stream (synthetic air, N_2/O_2, 80/20, Air Liquide, France) was electronically controlled by a massic flowmeter (Brooks® 5800, Lyon Vannes et Raccords, France) before being loaded with a defined amount of pollutant by passing through the mixing flask. The temperature of the thermoregulated bath, the gas flow rate and the geometric characteristics of the capillary tube determine the concentration of pollutant in the mixture [18]. For each pollutant, a specific cell was built and calibrated by weighing. The flow rate of the air stream was varied from 10 to 34 ml min^{-1}, corresponding to residence times in the photochemical reactor of 6 and 1.7 min, respectively. The pollutant concentration was varied from 900 to 5000 mg m^{-3}.

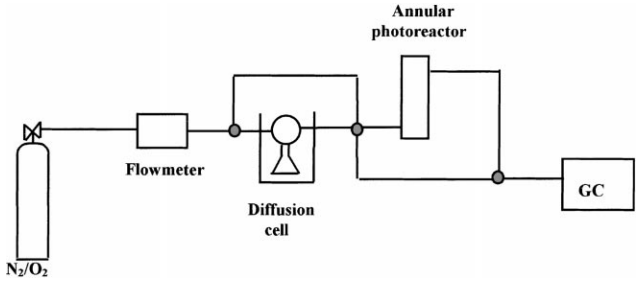

Fig. 1. Scheme of the experimental set-up.

The diffusion cell exit was linked to a continuous flow annular Pyrex reactor of 19.8 cm height, 4.1 cm external diameter and 3 cm internal diameter. The reactor could be used with two different types of lamps inserted in its central axis. Irradiations were carried out using either a medium pressure mercury lamp (TQ 150, Heraeus Noblelight, Germany), cooled by a slow stream of compressed air, or a xenon-chloride (XeCl) excimer lamp [19,20] of 25 cm in length and 3 cm of external diameter. The latter lamp emits a quasi-monochromatic radiation centered at 308 nm and is plugged into a ENI Model HPG-2 power supply operated at 150 W of electrical power and at a frequency of 200–220 kHz. When the excimer lamp was in use, the external tube of the lamp (Suprasil quartz) replaced the internal tube of the annular reactor. Incident photonic rates were determined by actinometry using potassium ferrioxalate as an actinometer [21,22]. A value of 1.6×10^{19} photon s^{-1} was obtained for the excimer lamp. The total rate of photons emitted by the Hg mercury arc (between 240 and 600 nm) was $1.1(\pm0.1)\times10^{19}$ photon s^{-1}. However, a Pyrex internal tube was used in the reactor and radiations of wavelength higher than 380 nm are not able to excite TiO_2. Therefore, the incident photon rate which may be absorbed by the photocatalyst (between 300 and 380 nm) was only $5.0(\pm0.5)\times10^{18}$ photon s^{-1} The temperature in the photochemical reactor was continuously monitored using a temperature sensor (HI 92804, HANNA Instruments) and was stable at approximately 30°C.

The tubing used for the various connections was either in copper or in PFA (Perfluoroalkoxy, Lyon Vannes et Raccords, France) and Swagelock joints (Lyon Vannes et Raccords) were employed.

2.2. Catalysts and chemicals

Supported catalysts were prepared in our laboratory from an amorphous TiO_2 gel deposited on porous quartz cylindrical beads (diameter=1.5 mm, length=10 mm) [23]. The specific surface area of the catalyst was 80 m^2 g^{-1}. An array of 38 photocatalytic beads (total TiO_2 mass of 107 mg) fixed on a non-porous quartz mesh (Coton Textiles pour Materiaux Innovants, France) was inserted into the reactor around the lamp well before each experiment. After irradiation, the catalysts were thermally regenerated (450°C). BU (99.9%) and BA (99%) were purchased from Aldrich and Prolabo, respectively, and used without further purification.

2.3. Analyses

The reactor exit was linked to a gas chromatograph (GC, Chrompack 9001) allowing continuous monitoring of gaseous products leaving the reactor. Injections were made using a 2.5 ml automatic injection loop heated up to 120°C. The GC was equipped with a CP-Sil-5 CB column (Chrompack) of 25 m length and 0.32 mm internal diameter.

Helium was used as a carrier gas. The injector temperature was 250°C and the flame ionization detector (901A Chrompack) was maintained at 300°C. The temperature gradient was fixed at 20°C min^{-1} between 40 and 200°C, with initial and final periods of 5 and 1 min, respectively. Some of the intermediates were also identified by GC-MS, using a Hewlett–Packard 5892 series 2 GC (column GE BPX5, 50 m, 0.22 mm, 0.25 μm) coupled to a mass spectrometer (Hewlett–Packard 597 lA). CO and CO_2 were detected by infrared spectroscopy (Perkin–Elmer 1760-x, DTGS detector). For this purpose, the gaseous sample was led through a 90 ml cell with CaF_2 windows.

3. Results and discussion

3.1. Adsorption

Adsorption of the pollutant is required for an efficient photocatalytic oxidation. We have therefore investigated the adsorption of gaseous BU and BA onto the TiO_2 catalytic beads (see Section 2.1 for the experimental set-up). This study was carried out in the photochemical reactor for various gas flow rates and pollutant concentrations. The evolution of the concentrations of BU and BA detected by GC in the gas stream at the reactor exit is shown in Fig. 2 (points at zero time correspond to the concentrations of pollutant in the gas stream at the entrance of the photochemical reactor).

Adsorption of both compounds was very efficient within the ranges of concentration and flow rate investigated, and was even more efficient for BU than for BA. Using the lowest flow rate (10 ml min^{-1}), the gas at the reactor exit did not contain any pollutant for 200 or 700 min in the case of BU and for 300 or 500 min in the case of BA (for gas phase concentrations of 5000 or 1500 mg m^{-3}, respectively). The corresponding saturation time was then approximately 900 or 2200 min for BU and about 1000 or 1600 min for BA. At higher flow rates (34 ml min^{-1}), the gas stream at the reactor exit contained some contaminant from the very beginning of the experiment. Under these conditions, the catalyst saturation time was shorter, 500 to 1200 min for BU (depending on the concentration) and 200 min for BA (5000 mg m^{-3}).

These results confirm the good adsorbing properties of the catalytic beads prepared [23] and show the efficient physisorption of BU and BA. The arrangement of the beads fixed onto the quartz mesh folded around the lamp well (Section 2.2) appears to be favorable. The amount of adsorbed pollutant at catalyst saturation depending on the nature of the compound, a maximum of 25 mg of BU and of 18 mg of BA could be adsorbed on the array of 38 catalytic beads under he experimental conditions used.

3.2. Photocatalytic degradations

Photocatalytic degradation experiments were carried out using a medium pressure mercury arc, but also, for the first time in the context of gaseous pollutant degradation, using a XeCl excimer lamp emitting at 308 nm. The electrical power of these two lamps is similar (Section 2.1), but in the case of the excimer lamp, the incident radiant power is concentrated within a narrow mission band at a favorable wavelength for absorption by TiO_2. The experiments were performed with thermally treated catalytic beads. Irradiation was started at the same time as the gas stream was introduced into the photochemical reactor, i.e. under conditions where the catalytic beads were not saturated with the model pollutant prior to irradiation. Therefore, irradiation times longer than needed for reaching adsorption equilibrium (Section 3.1 and Fig. 2) were used.

3.2.1. Irradiations using a medium pressure mercury arc

Under conditions of lowest concentration and flow rate, BU was totally mineralized (Fig. 3). FTIR study revealed only the presence of CO_2 and water vapor at the reactor exit and no products could be detected on the catalytic beads. Irradiation was carried out during 3000 min for controlling the continuity of the catalyst performance leading to total

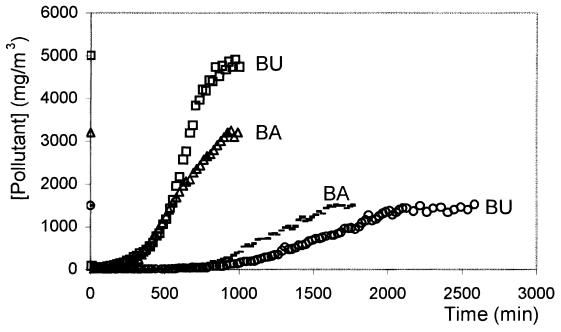

Fig. 2. Adsorption of BU and BA by an array of photocatalytic beads: evolution of pollutant concentration at the reactor exit as a function of time (gas flow rate: 10 ml min^{-1}); concentrations at reactor entrance: [BU]=1500 mg m^{-3}: open circles; [BU]=5000 mg m^{-3}: open squares; [BA]=1500 mg m^{-3}: dashes; [BA]=3200 mg m^{-3} open triangles.

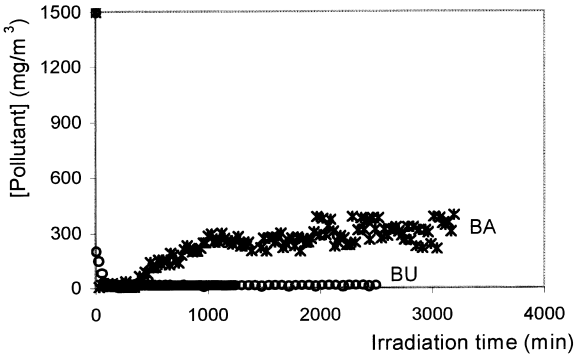

Fig. 3. Photocatalytic degradation of BU (open circles) and of BA (crosses): pollutant concentrations at the reactor exit as a function of irradiation time (medium pressure Hg arc, 1500 mg m^{-3} of pollutant in gas stream at reactor entrance, gas flow rate: 10 ml min^{-1}.

degradation of BU. Under the same conditions of concentration and flow rate, BA was not completely mineralized but a stationary state was reached after 1000 min, corresponding to 80% degradation.

When flow rate and concentration were increased (34 ml min^{-1} and 3200 or 5000 mg m^{-3}), rates of conversion decreased to 50% for BU and 30% for BA. This is due to the fact that a lower fraction of the starting material could be adsorbed on the catalytic beads (Fig. 2). A less efficient adsorption on TiO_2 also explains the slower degradation of BA compared to BU. The fact that stationary states are reached during photodegradation indicates that degradation rates are larger than desorption ones (adsorption–desorption equilibrium).

3.2.2. Irradiation using a XeCl excimer lamp

A higher efficiency of photodegradation should be observed when using the XeCl excimer lamp, due to the higher incident photonic rate emitted by this lamp in the wavelength range of TiO_2 absorption (Section 2.1). Therefore the experiments were performed under the less favorable conditions, i.e. for highest pollutant concentrations and gas flow rate. As expected, the conversion rates were found to increase significantly, from 50 to 85% for BU, and from 30 to 60% for BA (Fig. 4). The efficiency of TiO_2 photocatalysis may, hence, be significantly improved by replacing a medium pressure Hg arc by a XeCl excimer lamp of comparable size and electrical power.

3.3. Identification of intermediates and mechanism: 1-butanol

In order to establish the mechanism of the photocatalytic degradation of BU and BA, the evolution of the concentrations of the substrate and of the intermediates was followed by gas chromatography at the reactor exit during irradiation. However, in contrast to experiments described in Section 3.2, irradiation was started only after saturation of the catalytic

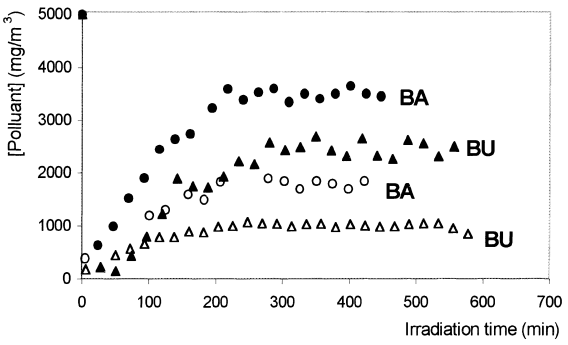

Fig. 4. Photocatalytic degradation of BU (triangles) and BA (circles): pollutant concentrations at the reactor exit as a function of irradiation time; open symbols: XeCl excimer lamp; full symbols: medium pressure Hg arc (5000 mg m^{-3} of pollutant in gas stream at reactor entrance, gas flow rate: 34 ml min^{-1}).

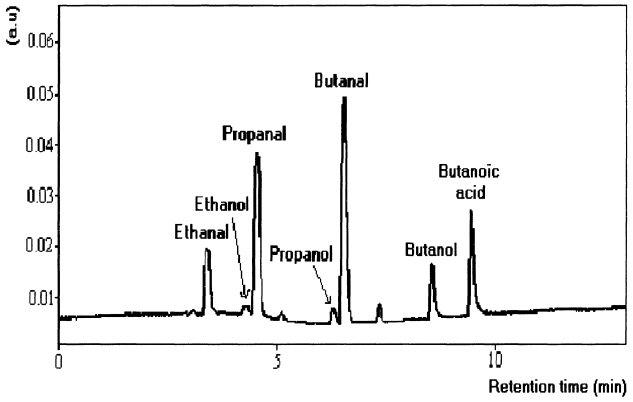

Fig. 5. Chromatogram obtained during the photocatalytic degradation of BU (1500 mg m^{-3} in gas stream at reactor entrance, gas flow rate: 10 ml min^{-1}, catalytic beads saturated with BU before irradiation).

beads by the pollutant, so that significant amounts of pollutant and intermediates reached the reactor exit. Quantitative determinations could be made under the following conditions: [BU]=1500 mg m^{-3}, [BA]=3200 mg m^{-3}, flow rate: 10 ml min^{-1}. Irradiations were performed using the medium pressure Hg arc.

3.3.1. Intermediates of the photocatalytic degradation of 1-butanol

Two compounds were previously detected and identified during investigations on the photocatalytic degradation of BU in the gas phase (see Section 1): butanal [12,14,15] and 1-butanoic acid [12]. During this work, five main products and five other compounds in trace amounts could be identified by GC analysis of the gas stream at the reactor exit (Fig. 5). The following main intermediates were formed: butanal, ethanal, propanal, 1-propanal, and butanoic acid (identified by GC-MS). In order to verify that butanal was the first intermediate in the reaction sequence of the photocatalytic degradation of BU, degradation of butanal was carried under the same conditions as used for BU. The same diffusion cell was used for both compounds since they have similar physical characteristics. The four other main intermediates already identified in the case of BU were again present, as well as the five products already observed as traces during BU degradation. One of the latter products could be identified as ethanol. Identifications were performed using GC-MS and confirmed by injection of original samples. GC-MS analysis did not show the presence of any traces of butane during the photocatalytic degradation of BU, in contrast to the assumptions of Blake and Griffin [14] and in agreement with the conclusions of Péral and Ollis [12]. Alcohol dehydration was not observed either during gas-phase heterogeneous photocatalytic oxidation of ethanol [24].

Fig. 6 shows the evolution of the concentrations of BU and of the main degradation intermediates in the gas stream at the reactor exit as a function of irradiation time. It should be noted that the evolution of concentrations as shown in

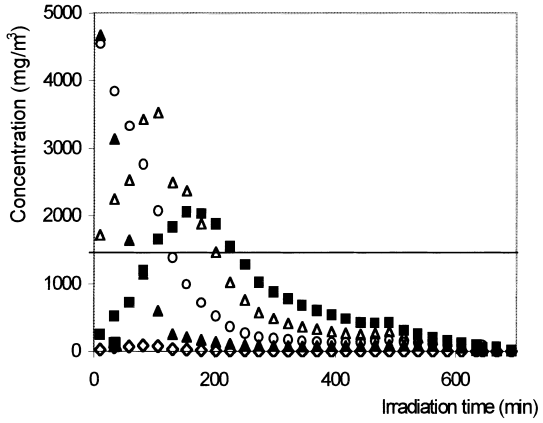

Fig. 6. Variation of the concentrations of BU (full triangles), butanal (open circles), 1-propanol (open diamonds), propanal (open triangles) and ethanal (full squares) in the gas stream at the reactor exit during the photocatalytic degradation of BU (1500 mg m^{-3} in gas stream at reactor entrance, gas flow rate: 10 ml min^{-1}, catalytic beads saturated with BU before irradiation).

Fig. 6 does not represent the actual conversion rate in the photochemical reactor. Under the experimental conditions used, the BU concentration decreased quickly and stabilized itself close to zero after 300 min. This stationary state was maintained for more than 3200 min.

At the beginning of the irradiation and during approximately 50 min of irradiation, the BU concentration at the reactor exit was higher than in the entering gas stream. This excess of BU can only be explained by partial desorption of this compound, adsorbed on the catalytic beads during the saturation process prior to irradiation. This desorption might be the consequence of a temperature increase, when the lamp was in operation, and/or irradiation might induce a photo-desorption phenomenon [25]. The concentrations of the intermediates (ethanal, propanal and butanal) also exceeded the concentration of BU in the entering gas stream (1500 mg m^{-3}, Fig. 6). It should be noted that the amount of BU adsorbed on the saturated catalytic beads before irradiation was high enough (25 mg) so that such a result was not unexpected.

Aldehydes desorbed faster than the corresponding alcohols. They were present in sufficient amounts at the reactor exit to be easily quantified, whereas the concentration of 1-propanol was very low and ethanol was only identified in trace amounts (Fig. 6). It was shown previously that alcohols and acids bind more efficiently to TiO_2 surfaces than aldehydes, e.g. the maximum amount of acetaldehyde adsorbed (mol g^{-1} of catalyst) was half the value for ethanol or acetic acid [24]. This result was interpreted in terms of a stronger binding of alcohols and carboxylic acids to the catalyst surface due to deprotonation upon adsorption at oxygen bridging sites [26]. In our experiments, butanal was present in large amount in the gas stream at the reactor exit at the beginning of the irradiation, its concentration decreasing to reach a stationary value of approximately 135 mg m^{-3} after 300 min of irradiation. Its decrease followed a pattern similar to that of BU, confirming that butanal is the first intermediate of the degradation of BU (Section 3.3.1). The concentration profiles of 1-propanol, propanal and ethanal are of the same type: their concentration increased during irradiation to reach a maximum (after 80, 100 and 170 min, respectively) and decreased to trace amounts after approximately 600 min of irradiation. Within experimental error, the stationary levels of BU and of the intermediates were independent of the fact that the catalytic beads were or not saturated with the substrate before irradiation.

3.3.1.1. Effect of water vapor. When the air stream was saturated with water vapor before entering the BU diffusion cell, saturation of the catalytic beads was faster, indicating that water adsorbs efficiently on the catalytic beads. However, although water occupies adsorption sites at the expense of the substrate, no significant effect on BU photodegradation was observed, as far as the stationary degradation level and the nature of the intermediates were concerned. Similar results were obtained by other authors in the case of trichloroethylene [27,28].

3.3.1.2. Importance of molecular oxygen. Degradation experiments carried out replacing air by nitrogen as a carrier gas confirmed the important role of molecular oxygen [29]. Under nitrogen, the products formed were the same as in the presence of air but the rate of conversion did not exceed 30%. It should be noted that the catalytic beads were not thoroughly degassed under vacuum before performing these experiments and that flushing the system with nitrogen was not sufficient to remove all traces of oxygen. Therefore, the results obtained may be explained by the presence of residual oxygen in the reaction system.

3.3.2. Mechanism of the photocatalytic degradation of 1-butanol

Our experimental results combined with previously reported data support the sequence of reactions proposed in Scheme 1 for the photocatalytic degradation of BU.

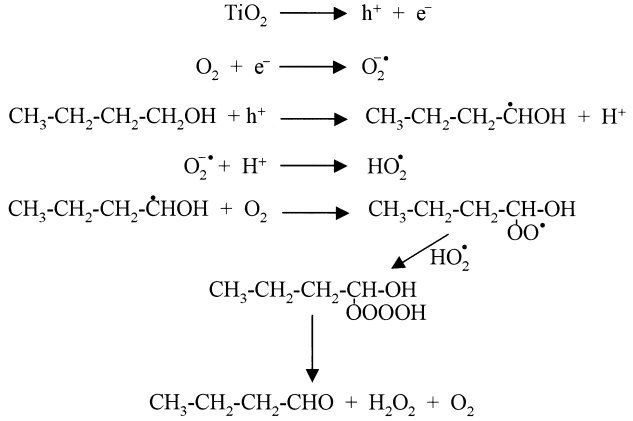

Scheme 1. Mechanistic scheme of the photocatalytic oxidation of BU.

Under irradiation, charge separation at the TiO_2 surface leads to the formation of hole–electron pairs (h^+–e^-). Adsorbed organic compounds can be directly oxidized by the holes [30] or, alternatively, holes may oxidize adsorbed water (formed during the degradation process or in the presence of water vapor) yielding hydroxyl radicals [31] which in turn oxidize the organic material. Oxidation of a primary alcohol by these highly oxidizing species would lead to the formation of a C-centered radical (ketyl radical $RC^{\bullet}(H)OH$) and trapping of the latter by molecular oxygen would result in the formation of a hydroxylated peroxyl radical. Heller et al. [29] have shown recently the important role played by molecular oxygen in the photocatalytic degradation of aliphatic compounds in the gas phase. Adsorbed oxygen efficiently traps the electrons from electron-hole pairs produced at the TiO_2 surface under irradiation, leading to the formation of superoxide anion ($O_2^{\bullet -}$) and its conjugated acid, the hydroperoxyl radical ($HO_2^{\bullet}$). The mechanism proposed involves reaction of the latter species with peroxyl radicals to form intermediate tetroxides ($RR'COOOOH$), as shown by von Sonntag and Schuchmann using pulse radiolysis experiments [32]. In the case of BU, decomposition of the intermediate tetroxide ($CH_3(CH_2)_2(H)C(OH)OOOOH$) would lead to the formation of butanal, hydrogen peroxide and oxygen (Scheme 1).

In agreement with such a mechanism, Fan et al. [33] could show that all the intermediates formed during the photocatalytic oxidation of TCE in the presence of $^{18}O_2$ incorporated $^{18}O_2$ and that the main intermediate oxidizing species involved were the $O_2^{\bullet -}$ and $HO_2^{\bullet}$. In contrast to previous assumptions, no evidence supporting the formation of hydroxyl radicals was found in these experiments. In the case of the photocatalytic degradation of BU at the gas–solid interface, we found similar results in the absence and in the presence of water vapor (vide supra, Section 3.3.1), supporting a major contribution of the holes to BU oxidation. The important role played by the holes has been demonstrated in the case of the oxidation of methanol using EPR spectroscopy [34].

The formation of butanoic acid may result from autooxidation of butanal [35] (Scheme 2). Butanoic acid may then be oxidized by the holes yielding carbon dioxide and the corresponding propyl radical. Trapping of the propyl radical by molecular oxygen yields the corresponding peroxyl radical which by dimerization forms the tetroxide. The latter decomposes to yield 1-propanol, propanal and oxygen (Scheme 2).

Note that oxidation of butanal by the holes (Reaction 1) followed by reaction of the radical thus formed with $HO_2^{\bullet}$. (Reaction 2) would lead to the corresponding peracid.

$$RCHO + h^+ \rightarrow RC^{\bullet}{=}O + H^+ \quad (1)$$

$$RC^{\bullet}{=}O + HO_2^{\bullet} \rightarrow RCOOOH \quad (2)$$

Similar reaction pathways as indicated in Schemes 1 and 2 lead to the formation of ethanol and ethanal by successive oxidation of 1-propanol, propanal and propanoic acid. Further degradation would yield methanol, formaldehyde and formic acid, and finally H_2O and CO_2 (detected by infrared spectroscopy).

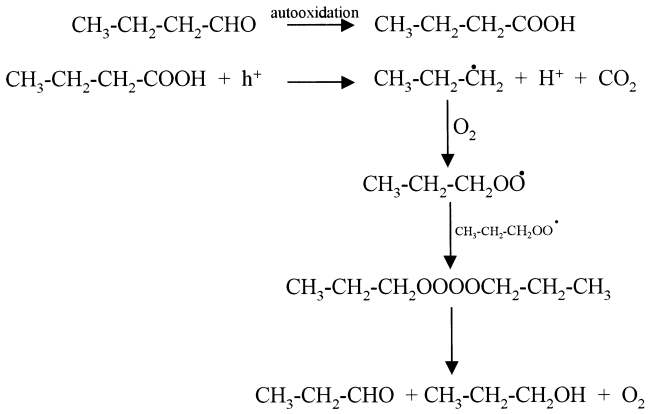

Scheme 2. Mechanistic scheme of the photocatalytic oxidation of butanal.

3.4. Identification of intermediates and mechanism: 1-butylamine

3.4.1. Intermediates of the photocatalytic degradation of 1-butylamine

In the case of BA, GC analysis of the gaseous mixture at the reactor exit showed the presence of at least six degradation products (Fig. 7). The formation of *N*-butylidene-1-butylamine was confirmed by GC-MS. Two other minor compounds could be identified as *N*-ethylidene-1-butylamine (compound 2, Fig. 7) and *N*-butylformamide which has a higher retention time than *N*-butylidene-1-butylamine. The presence of ammoniac in the gas stream at the reactor exit was shown using the Nessler reagent and formation of H_2O and CO_2 was confirmed by infrared spectroscopy.

During the degradation process, the concentration of *N*-butylidene-1-butylamine increased until a stationary state

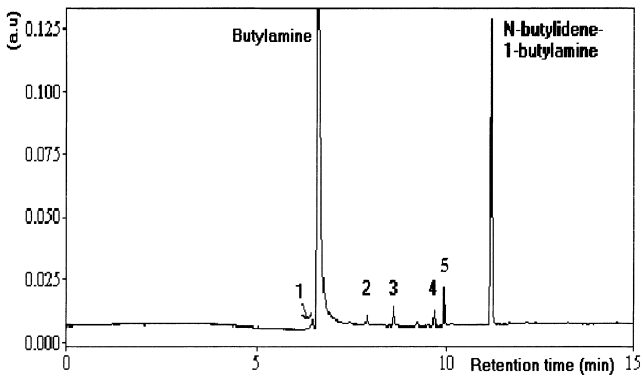

Fig. 7. Chromatogram obtained during the photocatalytic degradation of BA (3200 mg m^{-3} in gas stream at reactor entrance, gas flow rate: 10 ml min^{-1}, catalytic beads saturated with BA before irradiation).

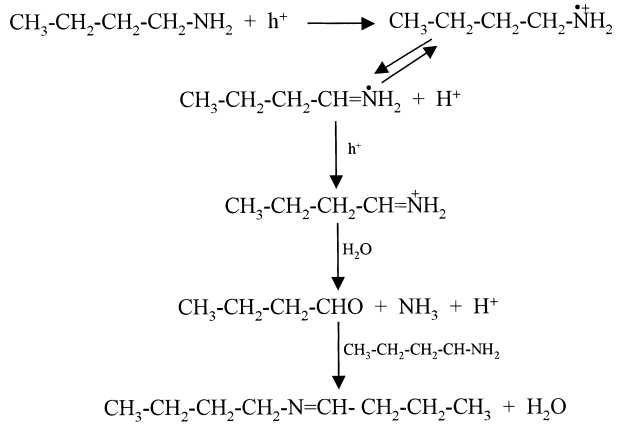

Scheme 3. Formation of *N*-butylidene-1-butylamine by photocatalytic oxidation of BA.

was reached after approximately 300 min. It should be noted that this imine was stable in the gas phase in spite of the presence of water. This product was formed at the beginning of the irradiation, whereas intermediates 1, 2, 3 and 5 could only be detected after 50 min of irradiation and intermediate 4 after 75 min (Fig. 7). The effects of water vapor and molecular oxygen on the photocatalytic degradation of BA were similar to those observed in the case of BU (Section 3.3.1).

3.4.2. Mechanism of the photocatalytic degradation of 1-butylamine

The mechanism of the photocatalytic degradation of BA might be similar to that proposed in the case of the electrochemical anodic oxidation of primary amines [36]. Such a mechanism would explain the formation of *N*-ethylidene-1-butylamine as an intermediate (Scheme 3). BA is oxidized by the holes at the catalyst surface yielding the corresponding imenium ion. In the presence of traces of water, ammoniac and butanal are formed, and reaction of the aldehyde with BA gives *N*-butylidene-1-butylamine. Besides, the presence of *N*-ethylidene-1-butylamine and *N*-butylformamide indicates that butanal was formed and was partially degraded (Scheme 2), aldehydes and acids successively formed reacting with BA to yield the two compounds mentioned above.

4. Conclusion

The photocatalytic degradation of 1-butanol and of 1-butylamine used as model pollutants was carried out using TiO_2 based catalysts prepared by a sol–gel method [23]. Their efficiency for the degradation of organic compounds in the gas phase was demonstrated and no deactivation of the photocatalyst during long irradiation periods was observed (more than 50 h). For the first time, a XeCl excimer lamp was used to irradiate TiO_2, and we could show that this lamp significantly increased the degradation rate of the model pollutants investigated, especially in the case of highly loaded gas streams (5000 mg m^{-3}, 34 ml min^{-1}). In all the cases investigated, experimental conditions leading to complete mineralization of the pollutant could be found.

Under conditions of partial degradation, several reaction intermediates could be detected and identified for both 1-butanol and of 1-butylamine. In the case of BU, 6 intermediates, instead of two in previous works [2,4,5], could be identified. Besides, we have shown that the presence of water vapor did not increase the degradation rate of BU and BA. Our experimental results support a degradation mechanism involving the holes formed under irradiation at the TiO_2 catalyst surface and superoxide anion as main oxidizing species.

Acknowledgements

The authors gratefully acknowledge financial support of this work by the ‘Conseil Régional de Midi-Pyrénées’, and technical support by G. Tayebi and J.C. Rouja. F.B.-M. thanks ADEME (Agence de l’Environnement et de la Maîtrise de l’Energie) for a grant.

References

[1] O. Legrini, E. Oliveros, A.M. Braun, Chem. Rev. 93 (1993) 671–698.
[2] D.F. Ollis, H. Al-Ekabi (Eds.), Photocatalytic Purification and Treatment of Water and Air, Elsevier, Amsterdam, 1993.
[3] S.B. Nielsen, T.K. Underbrink, E. Wong, B.M. Chow, VOC removal by air phase advanced oxidation processes, 9th Ozone World Congress Proceedings 1 (1989) 766–783.
[4] G.J. Johnson, T. Saarenvirta, P.M. Brown, J.A. Buckley, Industrial odour control, the Deodair process, 9th Ozone World Congress Proceedings 1 (1989) 387–401.
[5] K.R. Gütler, K. Kleinersmanns, Chemosphere 28 (1994) 1289–1298.
[6] A.M. Braun, L. Jakob, E. Oliveros, C.A.O. Nascimento, in: D. Volman, G.S. Hammond, D.C. Douglas (Eds.), Adv. Photochem., Vol. 18, 1993, pp. 235–313 and references cited therein.
[7] I. Gassiot, A.M. Braun, C. Baus, K. Schaber, 17th IUPAC Symposium on Photochemistry, Vol. 7, Sitges, Spain, 1998, p. 38.
[8] F. Benoit-Marquié, U. Wilkenhöner, A.M. Braun, E. Oliveros, M.T. Maurette, J. Phys. IV 9 (1999) 113–116.
[9] X. Fu, W.A. Zeltner, M.A. Anderson, in: P.V. Kamat, D. Meisel (Eds.), Semiconductor Nanoclusters, Studies in Surface Science and Catalysis, Vol. 103, Elsevier, Amsterdam, 1996, pp. 445–461.
[10] P. Pichat, Photochimie 94, Supplément à l’Actualité Chimique 7 (1994) 75.
[11] Y. Ohko, A. Fujishima, K. Hashimoto, J. Phys. Chem. B 102 (1998) 1724–1729.
[12] J. Péral, D.F. Ollis, J. Catal. 136 (1992) 554–565.
[13] K I. Suzuki, in: D.F. Ollis, H. Al-Ekabi (Eds.), Photocatalytic Purification and Treatment of Water and Air, Elsevier, Amsterdam, 1993, p. 421.
[14] N.R. Blake, G.L. Griffin, J. Phys. Chem. 92 (1988) 5697–5701.
[15] P. Pichat, P. Courbon, H. Disdier, M.N. Mozzanega, J.M. Herrmann, in: T. Seiyama, K. Tanabe (Eds.), Proceedings 7th Intern. Cong. Catal., Elsevier, Amsterdam, 1981, pp. 1498.
[16] K.I. Suzuki, S. Satoh, T. Yoshida, Denki Kagatu Qyobi Kogyo Butsuri Kagaku 6 (1991) 521–523.

[17] J.M. McKelvey, H.E. Hoelscher, Anal. Chem. 29 (1) (1957) 123.
[18] F.J. Debbrecht, D.T. Daugherty, E.M. Nell, Natur. Bur. Stand Spec. Publ. 519 (1979) 761–769.
[19] B. Eliason, U. Kogelschatz, H.J. Stein, EPA Newsletter 32 (1988) 29.
[20] B. Gellert, U. Kogelschatz, Appl. Phys. B 52 (1991) 14.
[21] A.M. Braun, M.T. Maurette, E. Oliveros, In Technologie Photochimique, Presses Polytechniques Romandes, Lausanne, 1986, p 70.
[22] F. Benoit-Marquié, Ph.D. Thesis, Photodégradation oxydative et catalytique de composés organiques en phase aqueuse et en phase gaze use, Universit Paul sabatier, Toulouse, France, 1997.
[23] F. Benoit-Marquié, C. Sarda, E. Puech-Costes, M.T. Maurette, E. Oliveros, J. Mat. Chem., submitted for publication.
[24] M.R. Nimlos, E.D. Wolfrum, M.L. Brewer, J.A. Fennel, G. Bintner, Environ. Sci. Technol. 30 (1996) 3102–3110.
[25] P. Pichat, J.M. Hermann, in: N. Serpone, E. Pelizzeti (Eds.), Photocatalysis Fundamentals and Applications, Wiley, New York, 1989, pp. 217–250.
[26] A.V. Kiselev, V.I. Lygin, Infrared Spectra of Surface Compounds, Wiley, New York, 1975.
[27] L.A. Dibble, G.B. Raupp, Catal. Lett. 4 (1990) 345–354.
[28] W.A. Jacoby, D.M. Blake, J.A. Fennell, J.E. Boulter, L.M. Vargo, M.C. George, S.K. Dolberg, J. Air & Waste Manag. Ass. 46 (1996) 891–898.
[29] J. Schwitzgebel, J.G. Ekerdt, H. Gerisher, A. Heller, J. Phys. Chem. 99 (1995) 5633–5638.
[30] W.H. Glaze, J.F. Kenneke, J.L. Ferry, Environ. Sci. Technol. 27 (1993) 177–184.
[31] D.F. Ollis, E. Pelizzetti, N. Serpone, Environ. Sci. Technol. 25 (1991) 1522–1529.
[32] C. Von Sonntag, H.P. Schuchmann, Angew. Chem. Int. Ed. Engl. 30 (1991) 1229–1253.
[33] J.F. Fan, J.C.S. Wong, J.T. Yates Jr., J. Am Chem. Soc. 118 (1996) 4686–4692.
[34] O.I. Micic, Y. Zhang, K.R. Cromack, A.D. Trifunac, M.C. Thurnauer, J. Phys. Chem. 97 (1993) 13284–13288.
[35] N.A. Clinton, R.A. Kenley, T.G. Traylor, J. Am. Chem. Soc. 97 (1975) 3746–3757.
[36] R. Lines, in: M.M. Baizer, H. Lund (Eds.), Organic Electrochemistry, Marcell Dekker, New York, 1983, pp. 463–468.